IAC-18

EFFECT OF EARTH-MOON PERTURBATION ON THE DEFLECTION OF TETHERED ASTEROID SYSTEMS

Luis O. Marchi[a]*, Flaviane C. F. Venditti[b], Arun K. Misra[c], Antonio F. B. A. Prado[a]

[a]*Graduate Course in Aerospace Space and Technology, National Institute for Space Research-INPE, 1758, Astronautas Avenue, Jardim da Granja, São José dos Campos-SP, Brazil,* marchi.luis@yahoo.com.br, antonio.prado@inpe.br
[b]*Arecibo Observatory/UCF, Route 625 Bo. Esperanza, Arecibo, Puerto Rico, USA,* fvenditti@naic.edu
[c]*Department of Mechanical Engineering, McGill University, 817 Sherbrooke Street, Montreal, Quebec, Canada*, arun.misra@mcgill.ca
* Corresponding Author

Abstract

The risk of impact of an asteroid with the Earth is not high, but the effects could be so tragic that this problem is an important one in astrodynamics. Several techniques are under consideration to avoid a collision of this type. One of the possibilities is to use a smaller asteroid to change the trajectory of a Potentially Hazardous Asteroid (PHA) that is on a collision course with the Earth by connecting them to each other with a tether. The physical reason of the deflection of the large asteroid is the displacement of the center of mass of the PHA by forming a new system composed of two asteroids and a tether. The dynamics is assumed to be planar, as a first study. Asteroids Bennu and Golevka are used for the numerical simulations, because they have small inclinations with respect to the Earth's orbit. The orbit deviations of the asteroids are computed for several initial conditions, but the main goal of the present work is to study in detail the influence of the Earth-Moon perturbation, before and after considering the presence of the tether and the smaller asteroid. It is shown that the dates and minimum distances are different from the results obtained neglecting the presence of the Earth and the Moon.

Keywords: Astrodynamics, Planetary Defense, Asteroid Deflection.

1. Introduction

In recent years, several celestial bodies with different shapes and sizes have been detected as they approach dangerously the orbit of the Earth. The threat of an impact with our planet has encouraged many studies on Potentially Hazardous Asteroids (PHA), which are objects with a minimum orbit intersection distance (MOID) of 0.05 AU or less, and an absolute magnitude (H) of 22.0 or brighter. In the literature, it is possible to find several techniques for the deflection of PHAs depending on the time available to plan and execute the mission. In 2022, for example, NASA's DART mission plans to perform the first kinetic impact experiment of a spacecraft on the moon of the double asteroid system Didymos [1]. In this work, a previously studied deflection method is considered, which involves in connecting the PHA to a smaller asteroid with a tether [2, 3]. The physical principle of the chosen technique is the displacement of the center of mass of the system, which changes the trajectory of the asteroid. The dynamics of all bodies involved are assumed to be planar, so the orbits of the PHA and the Earth around the Sun are assumed to be coplanar. Therefore, asteroids Bennu and Golevka were chosen for the numerical simulations in this paper because of the low inclinations of their orbits with respect to the orbit of the Earth. The tethered system is assumed to rotate with the angular velocity of the main body due to the constraint imposed by connecting the two bodies with a tether, which is assumed to be rigid and with negligible mass. The orbit deviations of the asteroids are obtained, but the focus of the present work is to analyze the influence of the Earth-Moon perturbation on the dynamics of the PHA and the PHA-tether-small asteroid system. It is expected that this effect becomes more evident in regions where there is more orbital interaction between the planet and these rocky bodies. The effects of the gravitational perturbation caused by the interaction between the binary asteroid system and the Earth-Moon system is studied with respect to the times and minimum distances of the close approaches. These effects are also quantified as the differences between the perturbed (by the tether and small asteroid) and unperturbed (asteroid alone) positions of the PHA after a certain time. The tether technique was adopted as a solution to avoid fragmentation debris that can be generated by the impact method, allowing to deflect the whole body without causing unpredictable consequences. In addition, another application would be to transfer these bodies closer to the Earth's orbit to explore them scientifically, as well as commercially, by mining important materials that are rare on the Earth and that exist in some asteroids. In this

regard, the ongoing Osiris-Rex mission plans to collect a small sample of the asteroid Bennu, which can possibly provide important information about the origin of the Solar System [4,5].

2. Literature Review

In total, more than 18000 NEAs are known, and about 90% of the NEAs larger than 1 km have already been found [6]. Because it is harder to detect smaller asteroids, the list grows each year with new technologies and new near-Earth objects (NEO) detection programs. The majority of objects entering the Earth's atmosphere are small enough to disintegrate before reaching the surface, but asteroids larger than about 30 meters can survive the atmospheric descent, possibly causing damages. To prevent a potential impact, some steps are necessary. First of all, it is necessary to find these bodies, which are done using optical and infrared telescopes. Next step is tracking and characterization, which can be done using ground radar observations from the Earth, that allow to refine the orbit with great precision, also giving details about the physical characteristics of the object, such as size, shape, spin state, and composition [7]. Having this information, the last step is to develop mitigation strategies in the event that a PHA is on the collision path with the Earth.

Several deflection methods have been proposed in the literature, for example: fragmentation of the asteroid using nuclear explosives or collision with a massive body [8]; use of solar energy with solar sails to cause a boost by the evaporation of the surface layers [9]; The use of the gravitational pull of a spacecraft near an asteroid to deflect it slowly, which is called the gravitational tractor method [10, 11].

In this work, a tether assisted technique is considered. Tethers are long space cables with several different applications. Some of the current studies using the concept of space tethers include the space elevator [12] and lunar elevator [13], use of tether satellite systems [14] for debris removal [15, 16] as well as using tethers for power and propulsion [17]. There have been several previous investigations on the application of tethers in asteroid deflection: the possibility of connecting a ballast mass brought from the Earth to a PHA has been examined, and also the optimization of the deflection by cutting the tether at an appropriate time [18, 19, 20, 21]. Considering the high number of small NEAs, it is proposed in this paper to use a smaller asteroid connected to a PHA by a tether, in order to alter the trajectory of an asteroid that poses a threat to the Earth. This technique would allow to use bigger masses if necessary, solving the problem of weight limitation when having to carry a mass from the Earth, which would increase significantly the fuel consumption during launch. It also would not cause fragmentation, like many other deflection methods. This technique was first studied considering only the gravitational attraction between the two bodies (PHA-ballast) [1,2,19,20,21], but here the effect of the Earth-Moon perturbation on the PHA-tether-smaller asteroid system is also considered.

3. Mathematical Formulation

The complete system can be seen in Figure 1. The inertial reference frame centered in the Sun (XY) is represented by the unit vectors $\{\hat{e}_1, \hat{e}_2\}$. The unit vectors $\{\hat{a}_1, \hat{a}_2\}$ correspond to the rotational reference frame (xy) with origin at the center of mass of the asteroid. The letters S, A, P and B represent the Sun, the center of mass of the PHA, the point of attachment of the tether in the large and in the smaller asteroid, respectively.

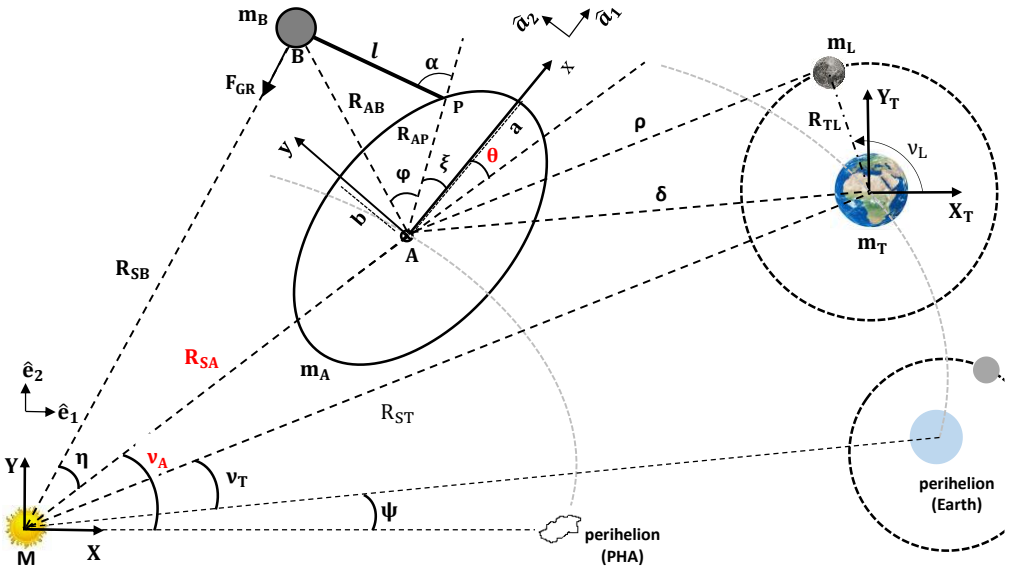

Fig. 1. Illustration of the physical model.

The other symbols used are: R_{SA}, the Sun-PHA distance; R_{ST}, the Sun-Earth distance; R_{SB}, the Sun-smaller asteroid distance; R_{AB}, the distance between the center of mass of the two asteroids; R_{TL}, the mean Earth-Moon distance; R_{AP}, the distance between the center of mass of the PHA and the point where the tether is attached to the PHA; δ, the PHA-Earth distance; ρ, the distance PHA-moon; l, the length of the tether; α, the angle between the tether and the PHA; ν_A, the true anomaly of the PHA; ν_T, the true anomaly of the Earth; ν_L, the true anomaly of the Moon; θ, the rotation angle of the PHA; φ, the angle between R_{AP} and R_{AB}; ξ, the angle between the point where the tether is fixed and the x-axis in the reference frame (xy); η, the angle between R_{SA} and R_{SB}; ψ, the difference between the lines of apsis of the Earth and the PHA; m_T, the mass of the Earth; m_L, the mass of the Moon; M, the mass of the Sun; m_A, the mass of the PHA and m_B, the mass of the smaller asteroid.

The positions of the asteroid (X_{SA}, Y_{SA}), of the Earth (X_{ST}, Y_{ST}) and of the Moon (X_{SL}, Y_{SL}), written in the inertial system (X, Y) are, respectively:

$$X_{SA} = R_{SA}cos(\nu_A) \quad (1)$$

$$Y_{SA} = R_{SA}sin(\nu_A) \quad (2)$$

$$X_{ST} = R_{ST}cos(\nu_T + \psi) \quad (3)$$

$$Y_{ST} = R_{ST}sin(\nu_T + \psi) \quad (4)$$

$$X_{SL} = X_{ST} + X_{TL} = R_{ST}cos(\nu_T + \psi) + R_{TL}cos(\nu_L) \quad (5)$$

$$Y_{SL} = Y_{ST} + Y_{TL} = R_{ST}sin(\nu_T + \psi) + R_{TL}sin(\nu_L) \quad (6)$$

where $\nu_L = \omega_L t = (2.64899\text{x}10^{-6}\ \text{rad/s})t$ is the angular position of the Moon (circular orbit) and $R_{TL} = 384400\ km$ is the distance between Earth and Moon.

The distance Sun-Asteroid (R_{SA}), Sun-Earth (R_{ST}) and Sun-Moon (R_{SL}) can be determined by basic geometry (distance between two points). From this, the distances PHA-Earth (δ) and PHA-Moon (ρ) are determine, respectively:

$$\delta = \sqrt{R_{ST}^2 - 2R_{ST}R_{SA}\cos(\nu_A - \nu_T - \psi) + R_{SA}^2} \quad (7)$$

$$\rho = \{R_{ST}^2 + R_{TL}^2 + R_{SA}^2 + 2[R_{ST}R_{TL}\cos(\nu_T + \psi - \nu_L) - R_{ST}R_{SA}\cos(\nu_T + \psi - \nu_A) - R_{TL}R_{SA}\cos(\nu_L - \nu_A)]\}^{1/2} \quad (8)$$

The total gravitational potential is given by the sum of four components according to Equation (9). The first one refers to the Sun-PHA interaction, the second to the Sun-Ballast interaction, the third to the Earth-PHA interaction, and the fourth to the Moon- PHA interaction. The spatial position of the additional mass (attached to the tether) does not change in time with respect to the PHA.

$$\begin{aligned} V_{TOT} &= V_{SUN/PHA} + V_{SUN/BALLAST} + V_{EARTH/PHA} + V_{MOON/PHA} \\ &= -\frac{GM}{R_{SA}} - GM\left[\frac{1}{R_{SA}} - \frac{R_{AB}}{R_{SA}^2}\cos(\theta + \xi + \varphi)\right] \\ &+ Gm_T\left[\frac{1}{\delta} - \frac{X_{SA}X_{ST} + Y_{SA}Y_{ST}}{R_{ST}^3}\right] \\ &+ Gm_L\left[\frac{1}{\rho} - \frac{X_{SA}X_{SL} + Y_{SA}Y_{SL}}{R_{SL}^3}\right] \end{aligned} \quad (9)$$

Asteroids Bennu and Golevka were chosen for this study because they have a small slope with respect to the plane of the ecliptic (model is two-dimensional). Table 1 shows the main physical parameters of these bodies.

Table 1. Orbital and physical parameters for Bennu and Golevka.

	Bennu	Golevka
mass (kg)	$7.8\text{x}10^{10}$	$2.1\text{x}10^{11}$
e	0.2038	0.6053
a (km)	$1.6851\text{x}10^{8}$	$3.7436\ \text{x}10^{8}$
i (deg)	6.035	2.2765
T (days)	436.6487	1445.9483
P_{rot} (h)	4.297	6.026

The total kinetic energy (translational plus rotational) of the system is given by:

$$\begin{aligned} T_{TOT} &= \frac{1}{2}\left[m_A(\vec{v}_{A_{XY}}.\vec{v}_{A_{XY}}) + m_B(\vec{v}_{B_{XY}}.\vec{v}_{B_{XY}}) + I_A(\dot{\theta} + \dot{\nu}_A)^2\right] \\ &= \frac{1}{2}(m_A + m_B)(\dot{R}_{SA}^2 + R_{SA}^2\dot{\nu}_A^2) \\ &+ \frac{1}{2}(\dot{\nu}_A + \dot{\theta})^2[m_B(l^2 + R_{AP}^2) + I_A] \\ &+ m_B(\dot{\theta} + \dot{\nu}_A)[lR_{PA}(\dot{\theta} + \dot{\nu}_A)\cos(\alpha) \\ &+ R_{PA}R_{SA}\dot{\nu}_A\cos(\xi + \theta) \\ &+ lR_{SA}\dot{\nu}_A\cos(\alpha + \xi + \theta) \\ &- \dot{R}_{SA}R_{PA}\sin(\xi + \theta) \\ &- l\dot{R}_{SA}\sin(\alpha + \xi + \theta)] \end{aligned} \quad (10)$$

where the moment of the inertia of the PHA-tether-ballast system is given by:

$$I_A = [(m_A + m_B)/(m_A + m_B)]R_{AB}^2 + (m_A + m_B)\left[\frac{m_B R_{AB}}{(m_A + m_B)}\right]^2 \quad (11)$$

From Equation (9), the total potential energy of the system is given by:

$$U_{TOT} = U_{SUN/PHA} + U_{SUN/BALLAST} + U_{EARTH/PHA} + U_{MOON/PHA} =$$

$$\begin{aligned}
&-m_A\frac{GM}{R_{SA}} \\
&+ m_A G m_T\left[\frac{1}{\sqrt{{R_{ST}}^2 - 2R_{ST}R_{SA}\cos(\nu_T + \psi - \nu_A) + {R_{SA}}^2}}\right] \\
&- m_A G m_T\left[\frac{R_{SA}R_{ST}\cos(\nu_A - \nu_T - \psi)}{{R_{ST}}^3}\right] \\
&+ m_A G m_L\left[\frac{1}{\sqrt{{R_{ST}}^2 + {R_{TL}}^2 + {R_{SA}}^2 + 2C_0}}\right] \\
&+ m_A G m_L\left[-\frac{R_{SA}R_{ST}\cos(\nu_A - \nu_T - \psi)}{C_1}\right] \\
&+ m_A G m_L\left[-\frac{R_{SA}R_{TL}\cos(\nu_A - \nu_L)}{C_1}\right] - m_B\left[\frac{GM}{R_{SA}}\right] \\
&+ m_B\left[GM\frac{R_{AB}}{R_{SA}^2}\cos(\theta + \xi + \varphi)\right] \quad (12)
\end{aligned}$$

where

$$\begin{aligned}
C_0 = {} & R_{ST}R_{TL}\cos(\nu_T + \psi - \nu_L) \\
& - R_{ST}R_{SA}\cos(\nu_T + \psi - \nu_A) \\
& - R_{TL}R_{SA}\cos(\nu_L - \nu_A)
\end{aligned}$$

and

$$C_1 = \left[{R_{ST}}^2 + {R_{TL}}^2 + 2R_{ST}R_{TL}\cos(\nu_T + \psi - \nu_L)\right]^{3/2}.$$

The Lagrangian of the system is given by the subtraction of the kinetic and potential energies ($\mathcal{L} = T_{TOT} - U_{TOT}$), where T_{TOT} and U_{TOT} are given by Eqs. (10) and (12), respectively.

The three ordinary differential equations of motion (function of time) are obtained from the Euler-Lagrange equations considering conservative system.

$$\frac{d}{dt}\left(\frac{\partial\mathcal{L}}{\partial\dot{q}_i}\right) - \frac{\partial\mathcal{L}}{\partial q_i} = 0, \qquad q_i = R_{SA}, \nu_A, \theta \quad (13)$$

where q_i are the generalized coordinates of the system.

For R_{SA}:

$$\begin{aligned}
&(m_A + m_B)\ddot{R}_{SA} \\
&- m_B(\dot{\theta} + \dot{\nu}_A)\dot{\theta}[R_{PA}\cos(\xi + \theta) + l\cos(\alpha + \xi + \theta)] \\
&- m_B(\ddot{\theta} + \ddot{\nu}_A)[R_{PA}\sin(\xi + \theta) + l\sin(\alpha + \xi + \theta)] \\
&+ \frac{GMm_A}{R_{SA}^2} - (m_A + m_B)R_{SA}\dot{\nu}_A^2 \\
&- m_B(\dot{\theta} + \dot{\nu}_A)\left(R_{PA}\dot{\nu}_A\cos(\xi + \theta) + l\dot{\nu}_A\cos(\alpha + \xi + \theta)\right) \\
&- m_B\left[-\frac{GM}{R_{SA}^2}\right] - m_B\left[\frac{2GMR_{AB}\cos(\varphi + \xi + \theta)}{R_{SA}^3}\right] \\
&+ Gm_Am_T\left[-\frac{\cos(\psi - \nu_A + \nu_T)}{R_{ST}^2}\right] \\
&+ Gm_Am_T\left[-\frac{2R_{SA} - 2R_{ST}\cos(\psi - \nu_A + \nu_T)}{2C_2}\right] \\
&+ Gm_Am_L\left[-\frac{R_{ST}\cos(\psi - \nu_A + \nu_T)}{C_1}\right] \\
&+ Gm_Am_L\left[-\frac{R_{TL}\cos(\nu_A - \nu_L)}{C_1}\right] \\
&+ Gm_Am_L\left[-\frac{2R_{SA}}{2(R_{SA}^2 + R_{ST}^2 + R_{TL}^2 + 2C_3)^{3/2}}\right] \\
&+ Gm_Am_L\left[\frac{2R_{ST}\cos(\psi - \nu_A + \nu_T)}{2(R_{SA}^2 + R_{ST}^2 + R_{TL}^2 + 2C_3)^{3/2}}\right] \\
&+ Gm_Am_L\left[\frac{2R_{TL}\cos(\nu_A - \nu_L)}{2(R_{SA}^2 + R_{ST}^2 + R_{TL}^2 + 2C_3)^{3/2}}\right] \quad (14)
\end{aligned}$$

where

$$C_2 = [R_{SA}^2 + R_{ST}^2 - 2R_{SA}R_{ST}\cos(\psi - \nu_A + \nu_T)]^{3/2}$$

and

$$\begin{aligned}
C_3 = {} & -R_{SA}R_{ST}\cos(\psi - \nu_A + \nu_T) \\
& - R_{SA}R_{TL}\cos(\nu_A - \nu_L) \\
& + R_{ST}R_{TL}\cos(\psi + \nu_T - \nu_L).
\end{aligned}$$

For θ:

$$\begin{aligned}
&-m_B\ddot{R}_{SA}\left(R_{PA}\sin(\xi + \theta) + l\sin(\alpha + \xi + \theta)\right) \\
&+ m_B\dot{\nu}_A\Big[\dot{R}_{SA}\left(R_{PA}\cos(\xi + \theta) + l\cos(\alpha + \xi + \theta)\right) \\
&- R_{SA}\dot{\theta}\left(R_{PA}\sin(\xi + \theta) + l\sin(\alpha + \xi + \theta)\right)\Big] \\
&+ I_A\left(\ddot{\theta} + \ddot{\nu}_A\right) \\
&+ m_B\Big[-\dot{R}_{SA}\dot{\theta}\left(R_{PA}\cos(\xi + \theta) + l\cos(\alpha + \xi + \theta)\right) \\
&+ \ddot{\theta}\left(l^2 + R_{PA}^2 + 2lR_{PA}\cos(\alpha)\right) \\
&+ \ddot{\nu}_A\left(l^2 + R_{PA}^2 + 2lR_{PA}\cos(\alpha) + R_{PA}R_{SA}\cos(\xi + \theta)\right. \\
&\left. + lR_{SA}\cos(\alpha + \xi + \theta)\right)\Big] \\
&- m_B(\dot{\theta} + \dot{\nu}_A)\Big[-\dot{R}_{SA}R_{PA}\cos(\xi + \theta) \\
&- l\dot{R}_{SA}\cos(\alpha + \xi + \theta) - R_{SA}R_{PA}\dot{\nu}_A\sin(\xi + \theta) \\
&- lR_{SA}\dot{\nu}_A\sin(\alpha + \xi + \theta)\Big] \\
&- \frac{GMm_BR_{AB}\sin(\varphi + \xi + \theta)}{R_{SA}^2} \quad (15)
\end{aligned}$$

For ν_A:

$$
\begin{aligned}
&\ddot{\nu}_A\left[m_B(2lR_{PA}\cos(\alpha)+l^2+R_{PA}^2)\right.\\
&+2m_BR_{SA}\left(l\cos(\alpha+\xi+\theta)+R_{PA}\cos(\xi+\theta)\right)\\
&\left.+(m_A+m_B)R_{SA}^2\right]\\
&+m_B\left[\ddot{\theta}\left(lR_{SA}\cos(\alpha+\xi+\theta)+2lR_{PA}\cos(\alpha)+l^2\right.\right.\\
&\left.+R_{PA}^2+R_{PA}R_{SA}\cos(\xi+\theta)\right)\\
&-\ddot{R}_{SA}\left(l\sin(\alpha+\xi+\theta)+R_{PA}\sin(\xi+\theta)\right)\\
&\left.-\dot{R}_{SA}\dot{\theta}\left(l\cos(\alpha+\xi+\theta)+R_{PA}\cos(\xi+\theta)\right)\right]\\
&+2\dot{\nu}_A\left[\dot{R}_{SA}\left(m_B\left(l\cos(\alpha+\xi+\theta)+R_{PA}\cos(\xi+\theta)\right)\right.\right.\\
&\left.+(m_A+m_B)R_{SA}\right)\\
&\left.-m_BR_{SA}\dot{\theta}\left(l\sin(\alpha+\xi+\theta)+R_{PA}\sin(\xi+\theta)\right)\right]\\
&+m_B\dot{\theta}\left[\dot{R}_{SA}\left(l\cos(\alpha+\xi+\theta)+R_{PA}\cos(\xi+\theta)\right)\right.\\
&\left.-R_{SA}\dot{\theta}\left(l\sin(\alpha+\xi+\theta)+R_{PA}\sin(\xi+\theta)\right)\right]\\
&+I_A\left(\ddot{\theta}+\ddot{\nu}_A\right)+Gm_Am_T\left[-\frac{R_{SA}\sin(\psi-\nu_A+\nu_T)}{R_{ST}^2}\right]\\
&+Gm_Am_T\left[\frac{R_{SA}R_{ST}\sin(\psi-\nu_A+\nu_T)}{\left(R_{SA}^2+R_{ST}^2-2R_{SA}R_{ST}\cos(\psi-\nu_A+\nu_T)\right)^{3/2}}\right]\\
&+Gm_Am_L\left[-\frac{R_{SA}R_{ST}\sin(\psi-\nu_A+\nu_T)}{C_1}\right]\\
&+Gm_Am_L\left[\frac{R_{SA}R_{TL}\sin(\nu_A-\nu_L)}{C_1}\right]\\
&+Gm_Am_L\left[-\frac{R_{SA}R_{ST}\sin(\psi-\nu_A+\nu_T)}{(R_{SA}^2+R_{ST}^2+R_{TL}^2+2C_3)^{3/2}}\right]\\
&+Gm_Am_L\left[-\frac{R_{SA}R_{TL}\sin(\nu_A-\nu_L)}{(R_{SA}^2+R_{ST}^2+R_{TL}^2+2C_3)^{3/2}}\right] \qquad (16)
\end{aligned}
$$

4. Results and Analysis

Numerical simulations were performed considering two asteroids: Bennu and Golevka. The step of the numerical integrator (RKF7) was considered fixed (1 minute) and the two main parameters measured were: deviation PHA-Earth (δ) and deviation between orbits with tether and without tether (Δ). The angles showed in Table 2 were used in all simulations, and the results are discussed next.

Table 2. Values of the angles used in the simulations.

Parameter	S.I.
α (deg)	10
ξ (deg)	30
ψ (deg)	0

In Figure 2, the orbits of each asteroid and the orbit of the Earth (blue) can be seen. The Sun is positioned at the center of the coordinate system (0,0). The line of the apsides of the Earth and the PHAs are assumed to be aligned with each other, so $\psi = 0°$. The beginning of the simulation takes place when the bodies are at the periapsis of their orbits, represented by the blue circle for the Earth, and the black and red circles for the PHAs. The tether was inserted after 1.2 simulation periods. This value was chosen randomly. In addition, Figure 2(a) shows that Bennu (black) has two points of close approach with the Earth, while Figure 2(b) shows only one region of approximation between Golevka (red) and the Earth.

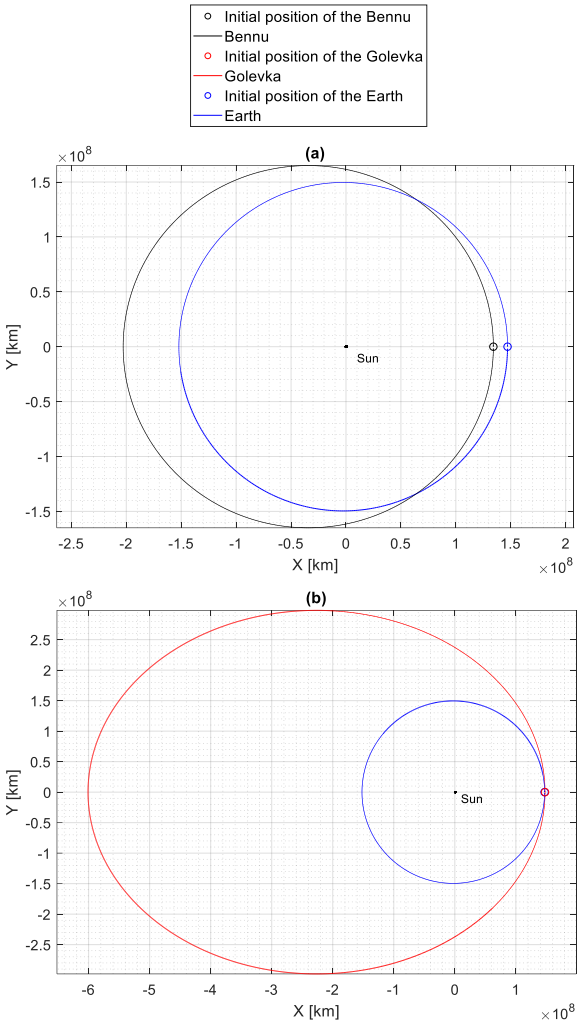

Fig. 2. Orbits of the bodies used in the simulations (a) Bennu (b) Golevka.

In Figure 3, the distance Earth-PHA per unit of radius of the Earth for 200 years of simulation is visualized. The maximum distance between Bennu and Earth is approximately 55000 R_E. The results show that there is a shift in time when the Earth-Moon system is included in the model. This shift increases with time, due to the cumulative effects of the perturbation. The black and blue lines are close, since they differ only by the presence of the tether and the ballast. This figure gives a general view of the evolution of those distances, but a closer view is necessary to understand better this problem. The minimum distances can be better visualized in Figure 4.

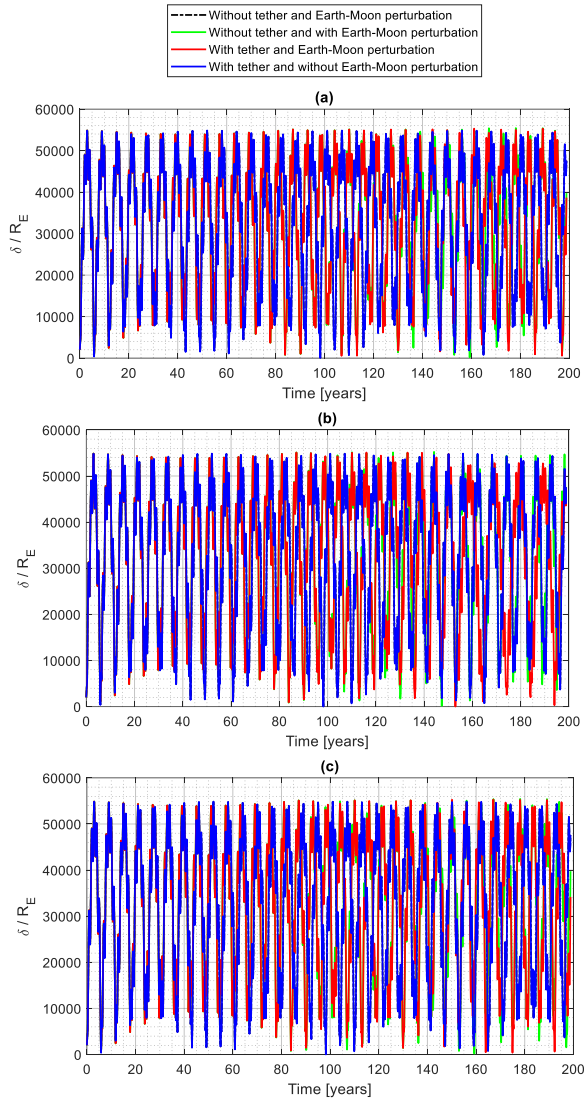

Fig. 3. Bennu-Earth distances considering mb/ma = 1/10000 for tether (a) 50 km (b) 500 km (c) 1000 km.

Figure 4 shows in more detail the closest approaches of the asteroid with the Earth, which are the more important results. Due to the initial configuration adopted for Bennu, the first approximation with risk of collision with Earth occurs in approximately 80 years, when considering the Earth-Moon perturbation. It is important to emphasize that Earth and asteroid start their motion with both of them at the periapsis of their orbits, and with both periapsis lines aligned. This is a configuration that occurs sometimes. Our study is focused in showing the effects of the Earth-Moon in this type of problem, but it is not concentrating in specific dates for the close approaches. Meaning that all the times showed here are measured with respect to this fictitious origin of time. In terms of real world, those times may occur before or after the times showed here, depending on the configuration of the bodies in the start time of the study.

The simulations made neglecting the effects of the Earth-Moon system in the trajectory of the asteroid reveal a very close approach in about 100 years of simulation. But, since the Earth-Moon is always present in the dynamics, this is a false warning of collision risk. Simulations including the presence of the ballast connected to the larger one by a tether show that this technique is useful. Note that the asteroid system passes by the Earth at a larger distance, compared to the trajectory of the asteroid alone.

The sub-figure showed in Figure 4(a), which has a tether of 50 km in length, indicates a new distance of close approach of about 16 R_E, which is about 0.5 Earth's radius more distant than the trajectory of the asteroid alone. The difference is not much, but it can be increased if even longer tethers are used. The sub-figure showed in Figure 4(b) is for a 500 km tether length, and it indicates a new distance of close approach of about 20 R_E, which is a shift of about 5 R_E compared to the trajectory of the asteroid alone. This is a considerable difference. Increasing the length of the tether to 1000 km (Figure 4(c)), the new close approach occurs at about 25 R_E, a significant increase of 10 R_E. These results show the importance of the technique used here to deviate the trajectory of an asteroid.

Considering the presence of the Earth-Moon in the system, there is no very close approach in the first 200 years of simulation. It means that the Earth-Moon perturbation deflected the asteroid much more efficiently than the tether and the smaller asteroid. Therefore, future studies should take this into account the better model of the system in order to avoid false alarm of collisions.

The closest approach in the first 200 years occurs around 159 years from the starting point of the simulation. The minimum distance reached is about 200 R_E, with no tether and ballast.

The use of the technique to deflect the asteroid is considerable for a tether length of 50 km (in 130 years), giving an increase in the closest distance of approach of 400 R_E, resulting in a minimum distance of 1800 R_E. For this case the use of tether kept the distance above 500 R_E for all simulation time (red curves). Using a tether with 500 km in length, the time of the closest approach goes to about 187 years, but the minimum distance decreases to near 220 R_E. It means that it is necessary to be careful with this technique, because in some situations it might not help to send the asteroid away from Earth in all the situations. It may even increase the risk of collision in some circumstances.

Increasing the tether length to 1000 km, the closest approach identified (green curve) in 159 years is replaced by two closer approaches, in 165 and 175 years (red curves). Both closest distances are above 400 R_E. In addition, in about 90 years the deviation was 470 R_E. It means that the maneuver is efficient in reducing the minimum distances of the approaches.

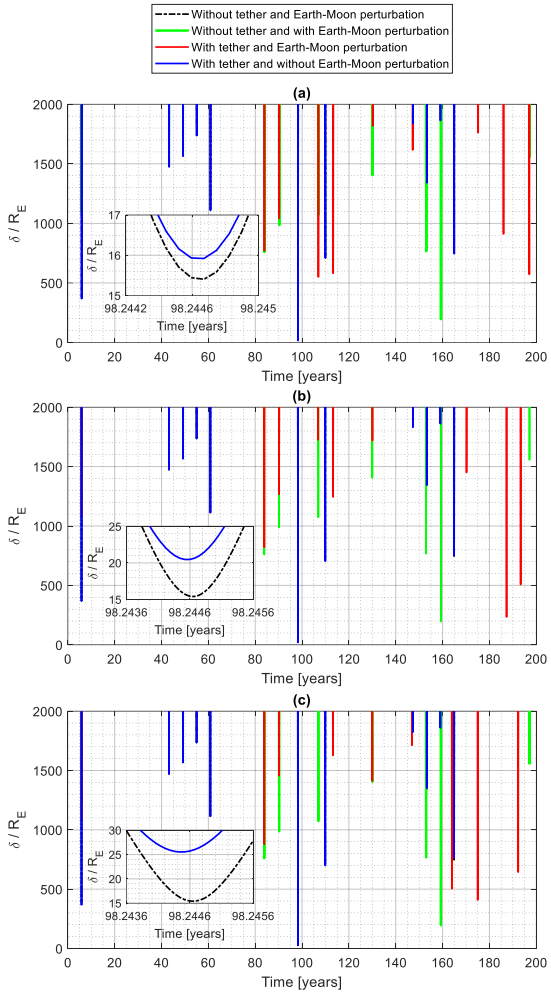

Fig. 4. Minimum distance Bennu-Earth considering mb/ma = 1/10000 for tether (a) 50 km (b) 500 km (c) 1000 km.

Next, we will analyze with more detail the effect of the tether and ballast in the motion of the asteroid (PHA). The Earth-Moon system is present in all the simulations. Figure 5 shows the deviation (Δ) between the trajectory considering the presence of the tether-ballast and the trajectory of the asteroid alone. The effects accumulate over the time and starts to be visible after 90 years of simulation. At this time there is a close approach with the Earth, which helps to increase the differences between the two orbits. The neighbor trajectories passing close to the Earth makes different swing-by, which makes them to increase their distance from each other. This is the reason of the increase in Δ after each close approach.

Figure 5(a), considering a tether of 50 km in length, shows a change in the behavior near 90 years and 107 years. In these moments the systems with tether and without tether have close approaches to the Earth (see Figure 4(a)), so increasing the amplitude of oscillations of Δ, as explained. It means that the perturbations generated in the trajectories are different, so the differences between the two orbits increase from this point until reaching the first maximum value in approximately 114 years. There are oscillations, because the point of the closest approach belongs to both orbits of both systems: the ones before and the ones after the close approach. So, the orbits systems will come closer periodically.

The same happens in Figure 5(b), which uses a 500 km tether. This case shows that the variation of Δ close to 84 and 90 years is amplified due to the increase in tether length (see Figura 4(b)). The similar effects of increasing Δ with close approaches occur here.

The influence of the passages near the Earth is clearly verified for the case where the tether is 1000 km long (Figure 5(c)). There is a visible change in the behavior of the curve at 84 years and 90 years, which is due to the close approach generated by the tether system (see Figure 4(c)). After that, there is a more evident modification in the behavior of the curve near 130 years, due to the approach of the trajectory of the asteroid alone and also of the tether-ballast system (1400 R_E) as shown in the Figure 4(c).

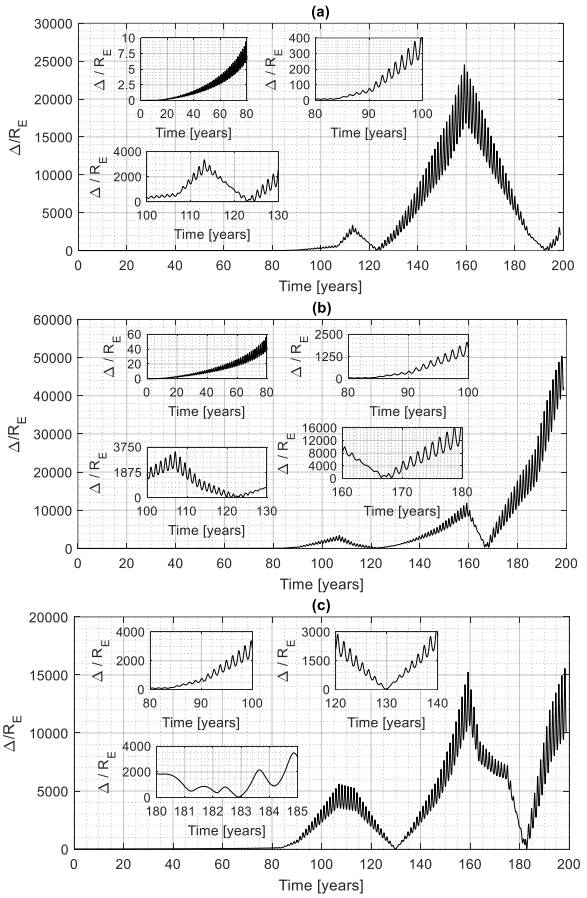

Fig. 5. Deviation (Δ) of Bennu in the presence of the tether-ballast system including the Earth-Moon perturbation for tether with (a) 50 km (b) 500 km (c) 1000 km.

In Figure 6, a general study of the evolution of the distances between Earth and Golevka is made, which the maximum is approximately 120000 R_E. This value is higher than the values reported for Bennu, due to the high eccentricity of Golevka's orbit. The black and blue lines are closer to each other, since they differ only by the presence of the tether and smaller asteroid. Green and red curves are near each other, for the same reason of differing only by the presence of the tether. They are shifted in time with respect to the blue/black lines, which shows the stronger effects of the presence of the Earth-Moon system in the dynamics. Those effects are much larger compared to the effects of the tether-ballast in the trajectory of the PHA. Table 1 shows that the period of Golevka is about 3.3 times longer than the orbital period of Bennu, which means that the interval between close approaches are much longer.

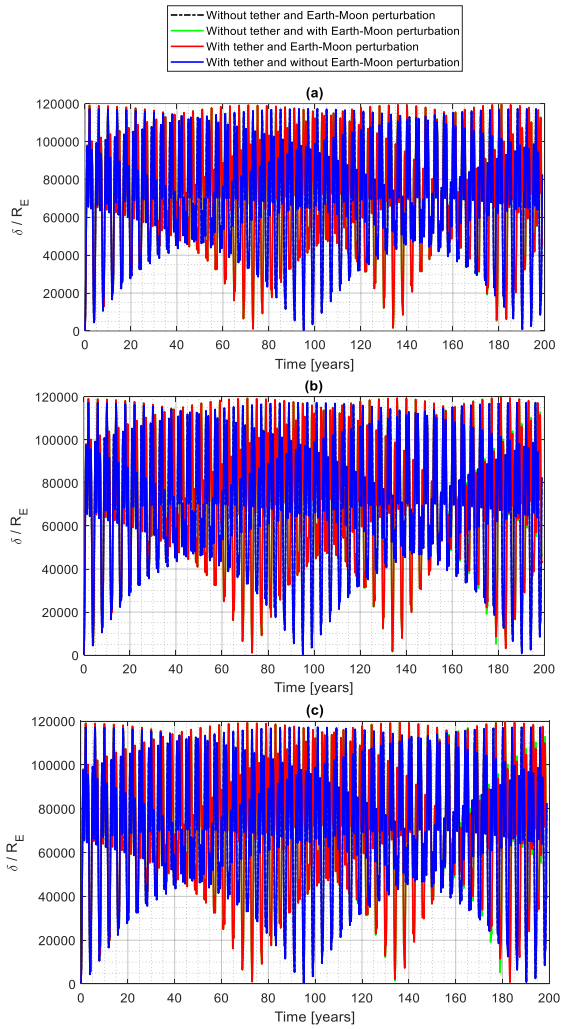

Fig. 6. Golevka-Earth distance considering mb/ma = 1/10000 for tether (a) 50 km (b) 500 km (c) 1000 km.

Figure 7 shows the closest approaches in more detail. Once again, the presence of the Earth-Moon in the system changes significantly the evolution of the closest approaches. If they are included in the dynamical equations, Golevka approaches the Earth again after about 73 years of simulation. Note that it starts close to the Earth, due to the initial conditions used in the simulations. This approach is not so close, with a minimum distance above 1000 R_E. The presence of a tether with a ballast does not help to deflect the PHA, instead, the approach is closer with the use of this technique. The differences are about 3.2 R_E for the 50 km tether, 18 R_E for the 500 km tether and 36 R_E for the 1000 km tether. The second approach to Earth is also very much influenced by the length of the tether. The passage around 134 years has a minimum distance close to 1600 R_E for the 50 km tether, 1850 R_E for the 500 km tether and above 2000 R_E (2200 R_E) for the 1000 km tether. These results confirm the importance of a detailed study before using this method. The results are quite different when the Earth-Moon is not included in the system.

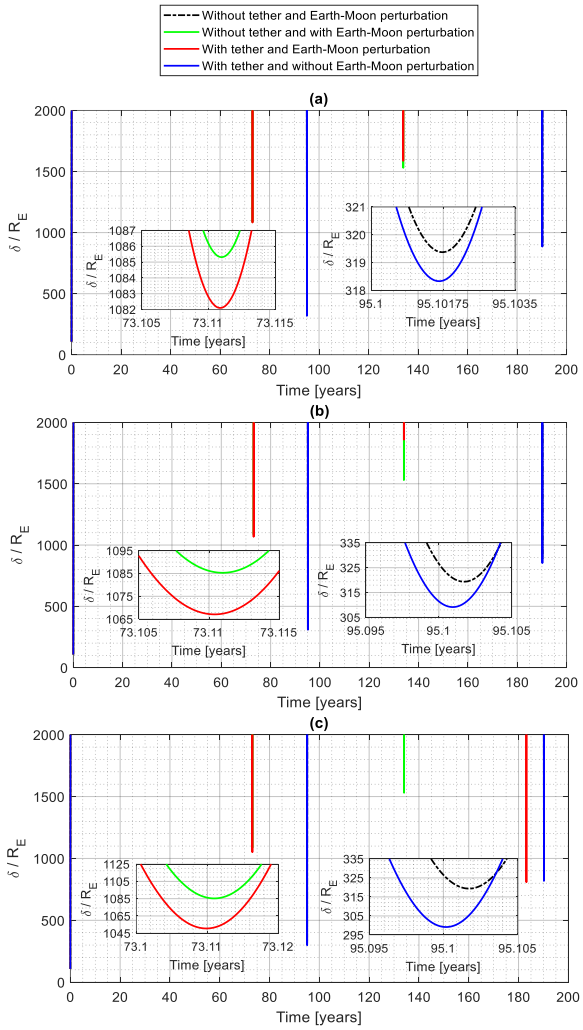

Fig. 7. Minimum distance Golevka-Earth considering mb/ma = 1/10000 for tether (a) 50 km (b) 500 km (c) 1000 km.

The black/blue lines give a false warning of collision risk in about 95 years of simulation, with a much closer minimum distance of 300 R_E. The simulations also showed that, due to the initial conditions, fixing the position of the ballast using the tether makes the PHA get closer to the Earth. These results may be desirable, for example, in missions where the purpose is scientific exploration of the asteroid. It means that the technique of fixing a ballast with a tether may have applications other than collision avoidance.

In Figure 8, we can observe that the non-uniform variation in Δ is associated with the successive swing-bys that happen with the Earth, as in the case of Bennu. The effects are accumulating in time and, after 80 years, it starts to be visible. At around 135 years the differences increase, because the passages near the Earth have different minimum distances when considering or not the presence of the tether with the ballast. Of course the differences increase for longer tethers, as can be seen in the graphs, because it generates larger variations in the Earth-Golevka minimum distances during the close approach.

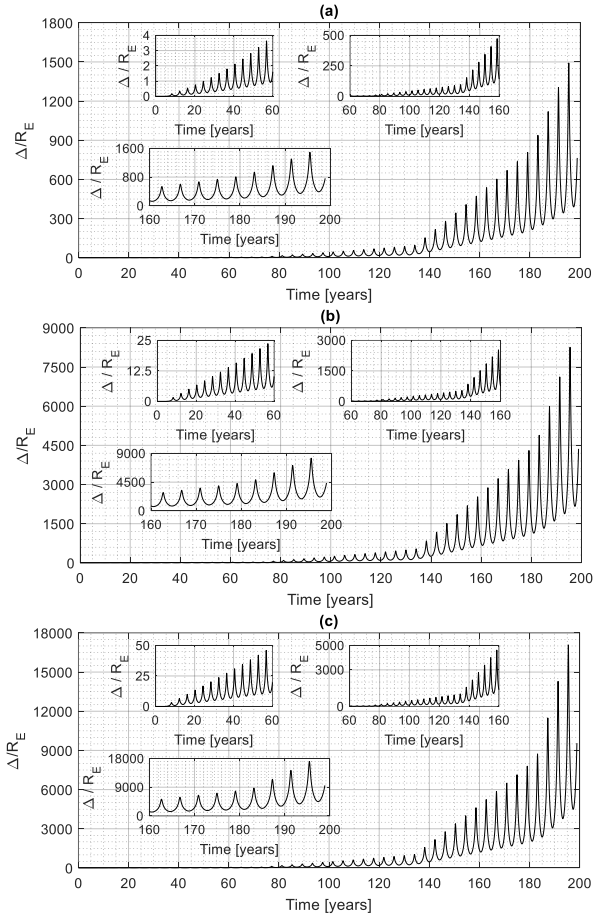

Fig. 8. Deviation (Δ) of Golevka in the presence of the tether-ballast system including the Earth-moon perturbation for tether with (a) 50 km (b) 500 km (c) 1000 km.

Next, Figure 9 shows the deviation (Δ) which is the difference between the trajectories of Bennu or Golevka considering the presence of the tether-asteroid, mb/ma = 1/10000, and the trajectory of the asteroid alone. For both asteroids, the effect of the Earth-Moon system on the trajectories is neglected. It is observed that, the longer the tether, the greater the deviations between the trajectories, as expected. In addition, the deviation is accentuated considering more eccentric orbits for the asteroid, as we see when comparing Figures 9(a) and 9(b). The oscillation in the curves is associated with the orbital period of each PHA.

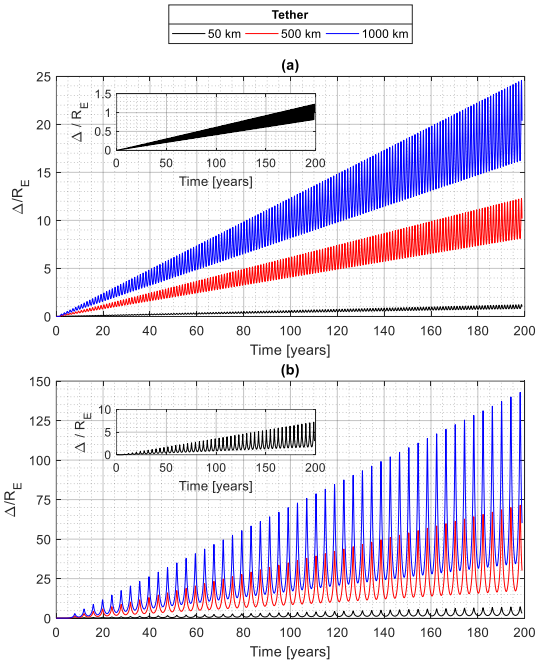

Fig. 9. Deviation (Δ) of Bennu (a) and Golevka (b) in the presence of the tether-ballast system (mb/ma = 1/10000). Earth-Moon perturbation is neglected.

5. Conclusions

The paper presented a study of the effects of the Earth-Moon perturbation on the dynamics of a system where a ballast is connected to a PHA with a tether, with the purpose of deflecting its trajectory from a possible impact with the Earth. Asteroids Bennu and Golevka were considered for the numerical simulations.

The presence of the Earth-Moon perturbation alters the dynamics of the system, even without the tether and the ballast attached. It changes the times and values of the minimum distances of the closest approach. There are also false warnings of collision risk if the Earth-Moon perturbation is neglected.

In general, including the Earth-Moon perturbation in the dynamical model modifies the trajectory of the asteroid much more than adding the tether and the ballast. Despite these differences, the use of a ballast reveals to be a technique useful in several conditions, but not

always. Therefore, detailed studies should be made to avoid situations where the use of this technique generates closer approaches compared to the trajectory of the PHA alone. In situations where the use of this technique is efficient, it increases the minimum distance of closest approach with the Earth by values up to the order of hundreds of the Earth's radius.

The differences between the orbits of the PHA alone and the system of asteroids attached by the tether increase with time, and the existence of jumps when passing close to the Earth are identified and measured. The increase of the deviation for greater length of the tether is also demonstrated and quantified.

The simulations for asteroid Golevka show an example when the use of a tether may reduce the minimum distances of the close approach, which is undesirable to deflect an asteroid from a possible collision, but can be interesting in missions with the purpose of scientific exploration or mining the asteroid.

Acknowledgements

The authors wish to express their appreciation for the support provided by grants# 406841/2016-0, 301338/2016-7, and 140501/2017-7 from the National Council for Scientific and Technological Development (CNPq), and grants# 2016/14665-2, 2016/18418-0, from São Paulo Research Foundation (FAPESP). We also are grateful for the financial support from the National Council for the Improvement of Higher Education (CAPES).

F. C. F. Venditti is supported by NASA's Near-Earth Object Observations Program at the Arecibo Observatory through grants no. NNX12AF24G and NNX13AF46G.

References

[1] Fahnestock, E.G., Kueppers, M. and Pravec, P., 2018. AIDA DART asteroid deflection test: Planetary defense and science objectives. Planetary and Space Science.

[2] Venditti. F. C. F., Misra. A. K. "Deflection of a Binary Asteroid System Using Tethers." 66th International Astronautical Congress, IAC-15-D4.3.1, 2015.

[3] Venditti. F. C. F., Marchi. L. O., Misra. A. K., Prado. A. F. B. A. "Dynamics of Tethered Binary Asteroid Systems." 49th Lunar and Planetary Science Conference, LPSC #1885, 2018.

[4] Berry. K., Sutter. B., May. A., Williams. K., Barbee. B. W., Beckman. M., Williams. B. (2013). OSIRIS-REx touch-and-go (TAG) mission design and analysis.

[5] Nolan. M. C., Magri. C., Howel., E. S., Benner. L. A., Giorgini, J. D., Hergenrother. C. W., Hudson. R. S., Lauretta. D. S., Margot. J. L., Scheeres, D. J. (2013). Shape model and surface properties of the OSIRIS-REx target Asteroid (101955) Bennu from radar and lightcurve observations. Icarus, 226(1), 629-640.

[6] http://www.cneos.jpl.nasa.gov/pd, (accessed 09.07.18).

[7] Naidu, S. P., Benner, L. A., Margot, J. L., Busch, M. W., & Taylor, P. A. (2016). Capabilities of Earth-based radar facilities for near-Earth asteroid observations. The Astronomical Journal, 152(4), 99.

[8] Ahrens, T. J., & Harris, A. W. "Deflection and fragmentation of near-Earth asteroids". Nature, 360(6403), 429-433, 1992.

[9] Melosh, H. J. "Solar asteroid diversion". Nature, 366, 21-22, 1993.

[10] Wie, B. "Dynamics and control of gravity tractor spacecraft for asteroid deflection". Journal of Guidance, Control, and Dynamics, 31(5), 1413-1423, 2008.

[11] Lu, E. T., & Love, S. G. "Gravitational tractor for towing asteroids". Nature, 438(7065), 177-178, 2005.

[12] Cohen, S. S., & Misra, A. K. (2007). "Elastic oscillations of the space elevator ribbon". Journal of Guidance, Control, and Dynamics, 30(6), 1711-1717.

[13] Burov, A. A., Guerman, A. D., & Kosenko, I. I. (2014). Tether orientation control for lunar elevator. Celestial Mechanics and Dynamical Astronomy, 120(3), 337-347.

[14] Misra, A. K. (2008). Dynamics and control of tethered satellite systems. Acta Astronautica, 63(11), 1169-1177.

[15] Ishige, Y., Kawamoto, S., & Kibe, S. (2004). Study on electrodynamic tether system for space debris removal. Acta Astronautica, 55(11), 917-929.

[16] Ivan der Heide, E. J., & Kruijff, M. (2001). Tethers and debris mitigation. Acta Astronautica, 48(5), 503-516.

[17] Sanmartin, J. R., & Lorenzini, E. C. Exploration of outer planets using tethers for power and propulsion. Journal of Propulsion and Power, 21(3), 573-576, 2005.

[18] French, D. B., & Mazzoleni, A. P. "Near-Earth Object Threat Mitigation Using a Tethered Ballast Mass". Journal of Aerospace Engineering, 22(4), 460-465, 2009.

[19] Mashayekhi, M. J., & Misra, A. K. "Tether assisted near earth object diversion". Acta Astronautica, 75, 71-77, 2012.

[20] Mashayekhi, M. J., & Misra, A. K. "Optimization of Tether-Assisted Asteroid Deflection". Journal of Guidance, Control, and Dynamics, 37(3), 898-906, 2014.

[21] Mashayekhi. M. J., Misra. A. K., Keshmiri. M. "Dynamics of a tether system connected to an irregularly shaped shaped celestial body". The Journal of the Astronautical Sciences, 63(3), 206-220, 2016.